

# Stochastic Rumor Spreading on a Spatial Network

A Study Based on the Daley–Kendall Model

Oumkalthoum M’HAMDI, Chaymae ED-Dyb, Zineb MIFTAH

Mathematical Models of Complexity

January 2026

## Abstract

Rumor spreading represents a fundamental example of complex collective dynamics driven by simple local interactions in social networks. This project investigates a stochastic, spatially explicit implementation of the Daley–Kendall (DK) rumor spreading model on a two-dimensional toroidal lattice. Agents occupy a  $40 \times 40$  toroidal grid ( $N = 1600$ ) and transition among ignorant, spreader, and stifler states. Spreaders attempt to transmit the rumor to a randomly chosen neighbor with probability  $p_{TS}$ , and may become stiflers with probability  $p_{SS}$  upon contacting already-informed neighbors. Outbreak size (final informed reach), persistence (lifespan to extinction), spatio-temporal patterns, and uncertainty are quantified using repeated Monte Carlo simulations, including a large ensemble of 10,000 replications per parameter setting.

Across the 10,000-run stochastic sweep at  $p_{TS} = 100\%$ , increasing stifling strongly reduces the final informed fraction from near saturation at low  $p_{SS}$  to  $\approx 39\%$  at  $p_{SS} = 100\%$ . Lifespan collapses from the non-extinct regime (capped at 5000 steps when  $p_{SS} = 0\%$ ) to  $\mathcal{O}(10^2)$  or less for  $p_{SS} \geq 10\%$ . A two-parameter sensitivity analysis over  $(p_{TS}, p_{SS})$  reveals a clear phase structure: high transmission and low stifling yield near-complete reach, whereas high stifling or low transmission lead to partial spread and short-lived outbreaks.

## 1 Introduction

Rumor spreading is a classical example of diffusion in social systems, relevant to the propagation of news and misinformation. Unlike epidemic contagion, rumor dynamics is strongly influenced by *novelty*: individuals may stop spreading once they realize the rumor is already widely known. Daley–Kendall (DK)-type models capture this mechanism by distinguishing three classes of agents: *ignorants* (unaware), *spreaders* (actively transmitting), and *stiflers* (aware but inactive).

Many analytical results for DK models rely on homogeneous mixing, where contacts are assumed random across the entire population. However, real interactions are structured and often local, which introduces correlations, clustering, and incomplete mixing. These effects can substantially change both the *final reach* (how many agents end up informed) and the *lifespan* (how long active spreading persists). Agent-based modeling is therefore well suited to study rumor dynamics under explicit spatial constraints.

This project examines a DK-type rumor model on a  $40 \times 40$  toroidal lattice ( $N = 1600$ ), where interactions occur locally between neighboring agents. Two parameters control the dynamics: the transmission probability  $p_{TS}$  (an ignorant becomes a spreader after contact with a spreader) and the stifling probability  $p_{SS}$  (a spreader becomes a stifler after contacting an already-informed neighbor). The analysis focuses on (i) outbreak size through final informed reach, (ii) persistence through steps to extinction, (iii) spatial organization of final states, and (iv) uncertainty quantified by repeated Monte Carlo simulations.

The report is organized as follows. Section 2 defines the agent-based lattice model, and Section 3 defines the measured quantities. Section 4 recalls the homogeneous-mixing (mean-field) DK model as an analytical baseline. Section 5 describes the simulation design, including a 10,000-replication sweep over  $p_{\text{SS}}$  and a two-parameter sensitivity analysis over  $(p_{\text{TS}}, p_{\text{SS}})$ . Section 6 presents results using phase diagrams, distributional summaries, and spatio-temporal diagnostics, followed by discussion and limitations in Section 7 and concluding remarks in Section 8.

## 2 Model Definition (Agent-Based DK on a Lattice)

### 2.1 Agent states

Each agent is in one of three discrete states:

- **Ignorant (0):** has not adopted the rumor (not spreading).
- **Spreader (1):** actively transmits the rumor.
- **Stifler (2):** has adopted the rumor but does not transmit it.

### 2.2 Spatial structure and neighborhood

Agents occupy a  $40 \times 40$  grid with periodic boundary conditions (toroidal topology), so there are no edges. Each agent interacts locally using a Moore neighborhood (up to 8 surrounding cells). At each interaction, a spreader selects *one* random neighbor (uniformly among available neighbors). Agents are stepped once per tick in random order (random sequential update).

### 2.3 Stochastic transition rules

Let  $p_{\text{TS}} \in [0, 1]$  denote the transmission probability and  $p_{\text{SS}} \in [0, 1]$  denote the stifling probability.

At each step:

1. Only **spreaders** initiate interactions.
2. A spreader picks one random neighbor:
  - If the neighbor is **ignorant**, a “times-heard” counter for that neighbor is incremented, and the neighbor becomes a **spreader** with probability  $p_{\text{TS}}$  (otherwise it remains ignorant).
  - If the neighbor is already informed (**spreader** or **stifler**), then the initiating spreader becomes a **stifler** with probability  $p_{\text{SS}}$ .

No other transitions occur: there is no spontaneous forgetting, no spontaneous stifling, and ignorants do not change state unless contacted by a spreader.

### 2.4 Initialization and stopping condition

A small number of agents are initialized as spreaders (5 spreaders seeded uniformly at random grid locations), with all others ignorant. The simulation stops when there are no spreaders remaining (extinction), or when a maximum number of steps is reached. In the reported experiments, a cap of 5000 steps is used; notably, when  $p_{\text{SS}} = 0\%$  the rumor does not extinct under these rules, so lifespan is reported as the cap value.

### 3 Measured Quantities

We compute the following metrics per simulation:

- **Final informed reach  $R$ :** number of agents that are non-ignorant (spreader or stifler) at termination.
- **Reach fraction  $R/N$ .**
- **Lifespan  $T$ :** number of steps until extinction (no spreaders), capped at 5000.
- **Final spatial pattern:** grid map of final states (ignorant/spreader/stifler).
- **Times-heard map:** number of times an agent was contacted while still ignorant. (When  $p_{TS} = 100\%$ , this is typically near-binary because ignorants convert on first contact.)

Uncertainty is quantified using repeated Monte Carlo replications, reporting means and confidence intervals.

### 4 Mean-Field Theoretical Description

Before presenting the spatial simulations, it is useful to recall the classical mean-field (homogeneous-mixing) Daley–Kendall (DK) model, which provides an analytical reference for rumor dynamics in a well-mixed population. In this idealized setting, contacts occur uniformly at random across the population (infinite-population limit), so spatial structure and local correlations are neglected.

Let  $x(t)$ ,  $s(t)$ , and  $r(t)$  denote the population fractions of ignorants, spreaders, and stiflers, respectively, with the conservation constraint  $x(t) + s(t) + r(t) = 1$ . Under homogeneous mixing, the DK dynamics can be written as

$$\frac{dx}{dt} = -\beta x s, \quad (1)$$

$$\frac{ds}{dt} = \beta x s - \gamma s (s + r), \quad (2)$$

$$\frac{dr}{dt} = \gamma s (s + r), \quad (3)$$

where  $\beta$  is an effective transmission rate and  $\gamma$  is an effective stifling rate. In a discrete-time lattice implementation where each spreader attempts one contact per step, a useful interpretation is that  $\beta$  and  $\gamma$  aggregate (i) the per-step contact rate and (ii) the per-contact probabilities  $p_{TS}$  and  $p_{SS}$ , so that the ratio  $\gamma/\beta$  is qualitatively aligned with  $p_{SS}/p_{TS}$  (up to contact-rate scaling).

A well-known final-size characterization is obtained in terms of the asymptotic ignorant fraction  $x_\infty = \lim_{t \rightarrow \infty} x(t)$ , which satisfies the implicit relation

$$x_\infty = \exp\left(-2(1 - x_\infty) \frac{\gamma}{\beta}\right). \quad (4)$$

In the balanced-rate case  $\gamma = \beta$ , numerical solution of (4) yields  $x_\infty \approx 0.203$ , implying that approximately  $1 - x_\infty \approx 79.7\%$  of the population eventually becomes informed under mean-field assumptions.

The remainder of this report focuses on the spatial, stochastic version implemented on a lattice, where neighbor-based interactions and finite-size fluctuations can lead to departures from homogeneous-mixing predictions.

## 5 Experimental Design

### 5.1 Large stochastic sweep over stifling (10,000 runs per level)

We run 10,000 independent simulations for each stifling level

$$p_{\text{SS}} \in \{0\%, 10\%, 20\%, \dots, 100\%\},$$

using fixed transmission  $p_{\text{TS}} = 100\%$ . For each level we summarize the distribution of reach and lifespan, and compute a 95% confidence interval for the mean reach.

### 5.2 Two-parameter sensitivity analysis (phase diagrams)

We run a phase-diagram experiment over:

$$p_{\text{TS}} \in \{10\%, 25\%, 50\%, 75\%, 100\%\}, \quad p_{\text{SS}} \in \{10\%, 25\%, 50\%, 75\%, 100\%\}.$$

For each grid cell  $(p_{\text{TS}}, p_{\text{SS}})$ , 500 Monte Carlo replications are performed, and we record mean final informed reach and mean lifespan. This produces two heatmaps (reach and lifespan), interpreted as an empirical “phase diagram” of the rumor dynamics.

## 6 Results

### 6.1 Stochastic sweep (10,000 runs): reach and lifespan vs stifling

Table 1 summarizes the 10,000-run results. Two robust trends appear:

1. **Final reach decreases monotonically with stifling.** With  $p_{\text{TS}} = 100\%$ , mean reach is near saturation for low stifling, but falls sharply as  $p_{\text{SS}}$  increases, reaching  $\approx 39\%$  at  $p_{\text{SS}} = 100\%$ .
2. **Lifespan collapses once  $p_{\text{SS}} > 0\%$ .** When  $p_{\text{SS}} = 0\%$ , spreaders never convert to stiflers, so extinction does not occur and the simulation is truncated at 5000 steps. For  $p_{\text{SS}} \geq 10\%$ , extinction occurs rapidly (tens to  $\sim 100$  steps).

$p_{SS}$	mean reach	reach (%)	CI <sub>95</sub> low	CI <sub>95</sub> high	mean steps
0%	1600.00	100.00	1600.00	1600.00	5000.00
10%	1599.54	99.97	1599.34	1599.74	91.14
20%	1590.38	99.40	1589.94	1590.82	54.09
30%	1562.32	97.64	1561.50	1563.14	44.29
40%	1516.10	94.76	1514.92	1517.28	41.97
50%	1450.61	90.66	1449.07	1452.15	42.27
60%	1362.66	85.17	1360.34	1364.98	45.91
70%	1243.40	77.71	1239.50	1247.30	50.03
80%	1070.90	66.93	1064.36	1077.44	51.92
90%	849.77	53.11	841.07	858.47	49.28
100%	627.43	39.21	618.61	636.25	42.82

Table 1: Stochastic sweep over stifling probability (10,000 simulations per setting) with  $p_{TS} = 100\%$ . Mean reach counts agents that are non-ignorant at termination. Lifespan is steps until extinction (no spreaders), capped at 5000 steps.

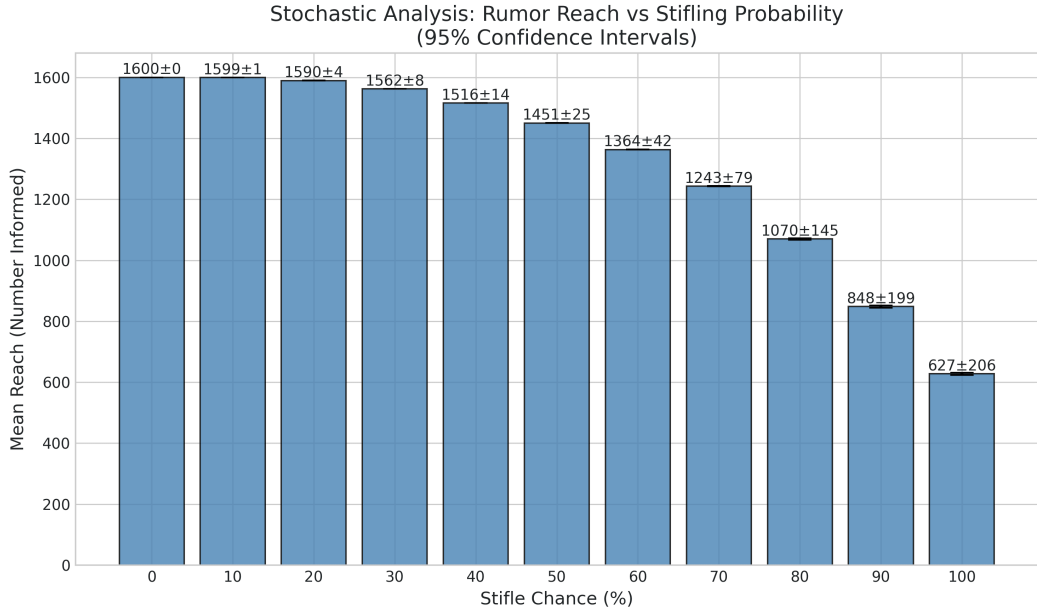


Figure 1: Mean reach vs stifling probability with 95% confidence intervals (large Monte Carlo ensemble).

## 6.2 Distributional uncertainty: variability increases at high stifling

Beyond mean trends, the distributions broaden as  $p_{SS}$  increases. When stifling is low, reach is tightly concentrated near saturation. At high stifling, extinction occurs earlier and local spatial clustering matters more, leading to much larger run-to-run variability in how far the rumor penetrates.

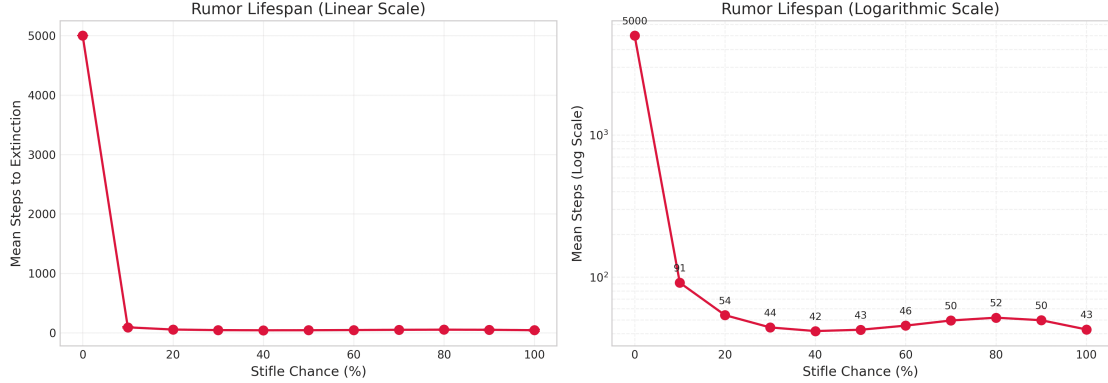


Figure 2: Mean lifespan (steps to extinction) vs stifling probability, shown on linear and log scales. The point at  $p_{SS} = 0\%$  is capped at 5000 steps because extinction does not occur under the model rules.

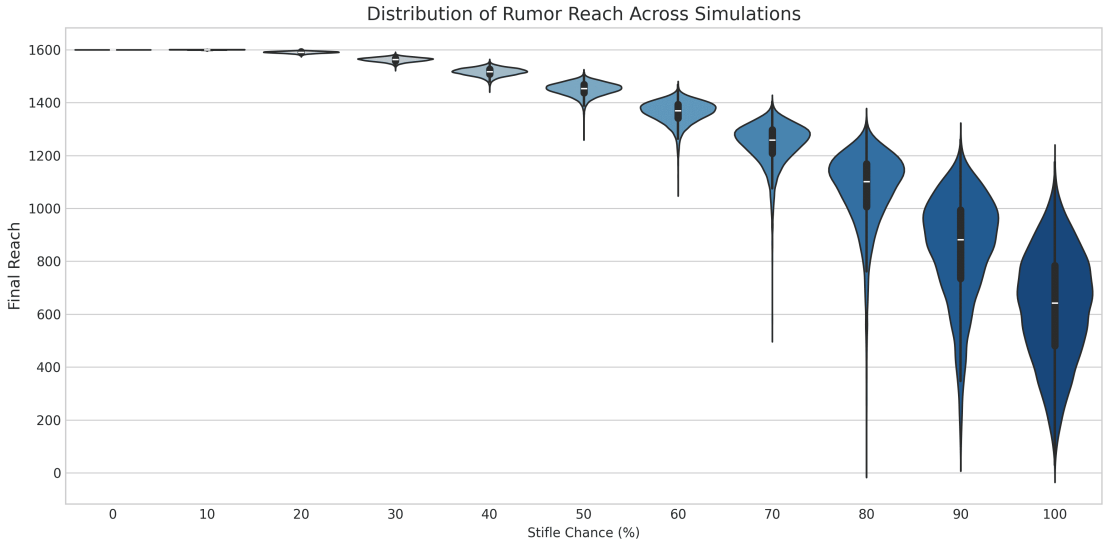


Figure 3: Distribution of final reach across simulations as a function of stifling probability (violin plots).

### 6.3 Two-parameter phase structure (transmission vs stifling)

Figure 5 presents phase diagrams for mean reach and mean lifespan across  $(p_{TS}, p_{SS})$ . The diagrams show an intuitive structure:

- **High transmission and low stifling** yields near-complete penetration ( $R \approx N$ ).
- **High stifling** suppresses penetration even when transmission is strong.
- **Low transmission** yields limited reach and typically shorter outbreaks, with outcomes sensitive to early stochastic branching.

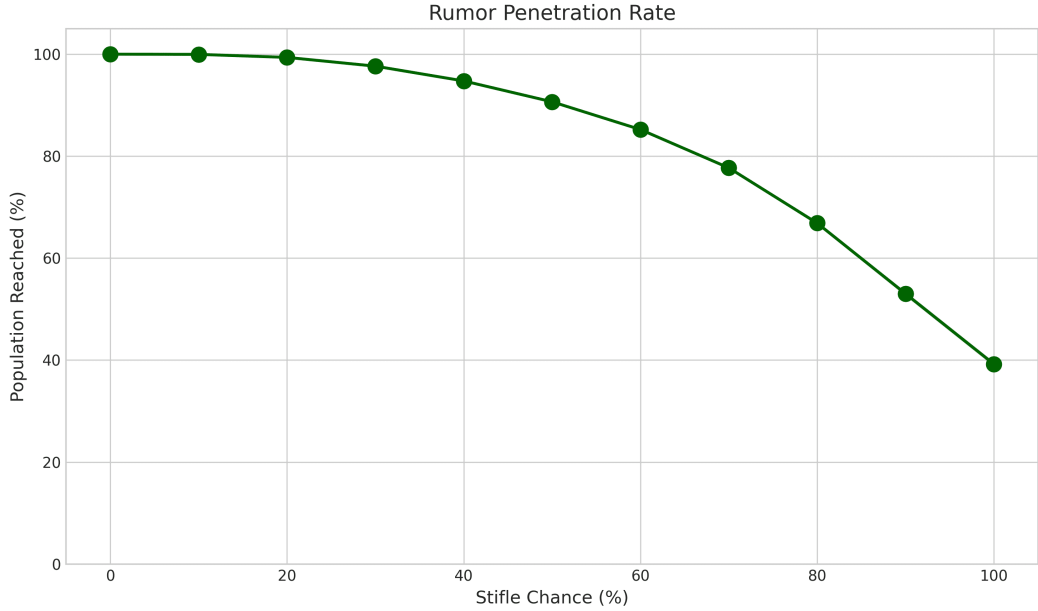


Figure 4: Rumor penetration rate (fraction reached) vs stifling probability.

#### 6.4 Spatial patterns of final states

Spatial snapshots reveal how local interactions shape outcomes. For low or moderate stifling, most of the grid becomes informed (often dominated by stiflers at the end). As stifling increases, larger connected regions of ignorants can remain, indicating that the rumor fails to cross certain spatial gaps before the remaining spreaders stifle.

#### 6.5 Times-heard maps

The times-heard maps show where ignorants were contacted while still ignorant. In the  $p_{TS} = 100\%$  examples plotted here, most nonzero entries are near 1 (conversion on first contact), so the maps primarily visualize the *spatial footprint* of the outbreak. For  $p_{TS} < 100\%$ , this diagnostic also captures genuine repeated exposures (multiple contacts without conversion).

#### 6.6 Temporal dynamics: spreader population over time

The temporal curves show that increasing stifling reduces both the peak number of spreaders and the duration of spreader activity. When  $p_{SS} = 0\%$ , spreaders do not convert to stiflers, and the spreader population remains high indefinitely (until the imposed cap). For  $p_{SS} > 0\%$ , the spreader population rises initially, then collapses as stifling interactions accumulate.

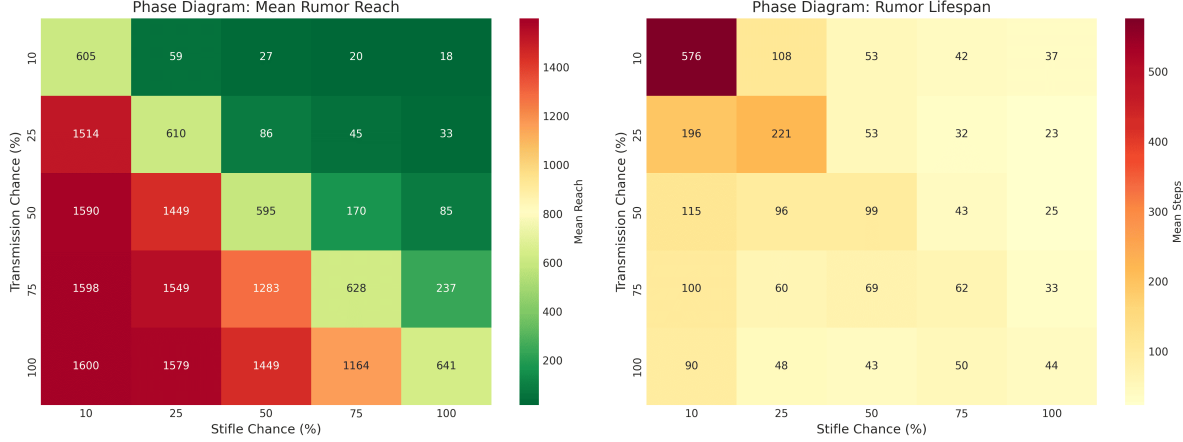


Figure 5: Phase diagrams over transmission probability  $p_{TS}$  and stifling probability  $p_{SS}$ : (left) mean final reach, (right) mean lifespan.

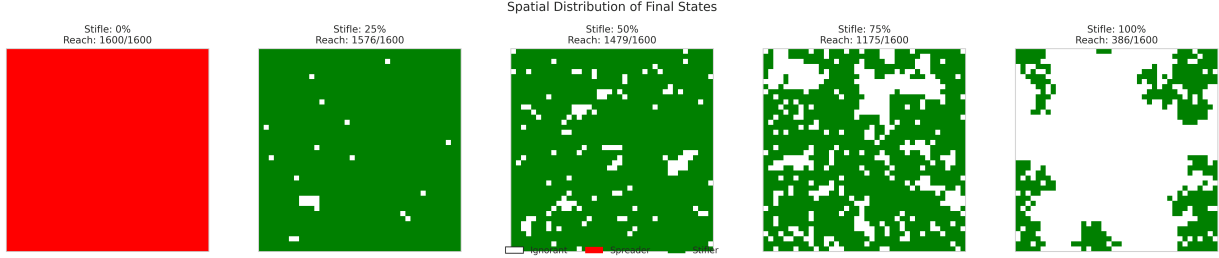


Figure 6: Spatial distribution of final states for selected stifling levels (example realizations). White: ignorant, red: spreader, green: stifler.

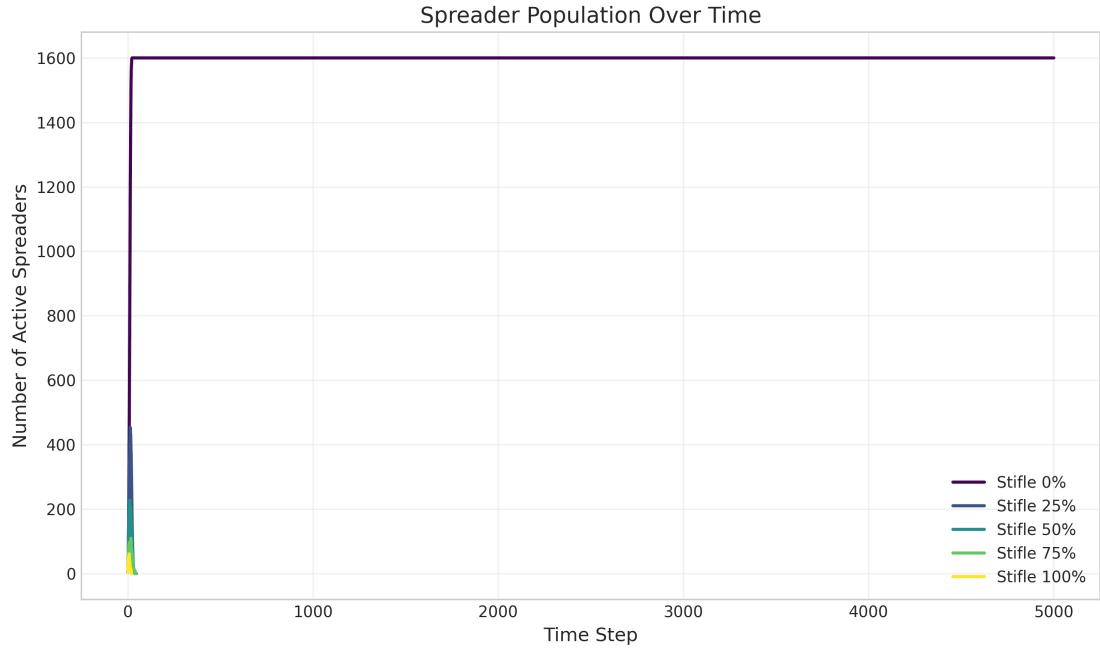


Figure 8: Spreader population over time for multiple stifling levels (illustrative trajectories).

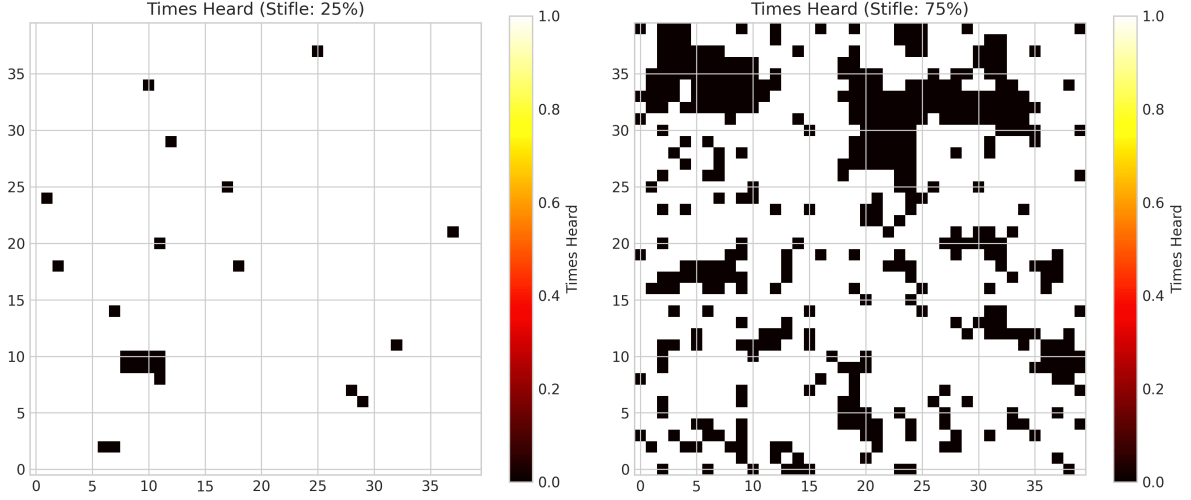


Figure 7: Times-heard maps for two stifling levels (example realizations,  $p_{TS} = 100\%$ ).

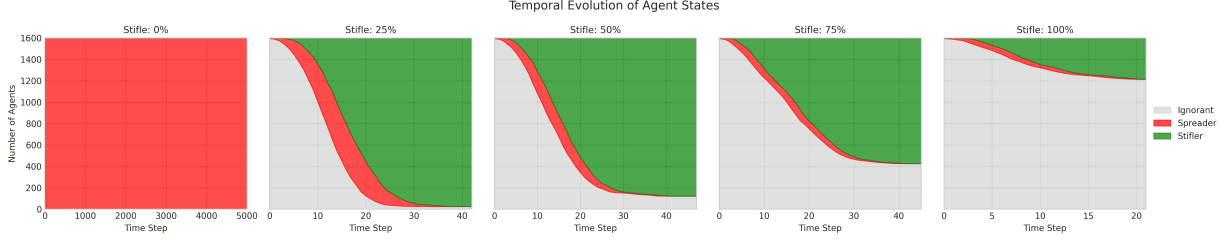


Figure 9: Temporal evolution of ignorant/spreader/stifler counts for selected stifling levels (illustrative trajectories).

## 7 Discussion and Limitations

- **Non-extinction at  $p_{SS} = 0\%$ :** because spreaders never convert to stiflers, extinction does not occur; lifespans reported at 5000 are truncation artifacts rather than true extinction times.
- **Locality and clustering:** the lattice topology breaks the homogeneous-mixing assumption and can reduce final reach by preventing the rumor from efficiently crossing spatial gaps.
- **One-contact-per-step rule:** each spreader contacts one neighbor per step, which sets an effective contact rate and influences timescales. Different contact rules would change lifespans and possibly the phase structure.
- **Finite size effects:** with  $N = 1600$ , stochastic fluctuations are important in the high-stifling regime, where outcomes depend strongly on early local branching and extinction events.

## 8 Conclusion

We implemented a DK-type rumor model on a  $40 \times 40$  toroidal lattice and performed extensive Monte Carlo analysis, including a 10,000-run sweep over stifling probability and a two-parameter

sensitivity study over transmission and stifling. The results show a strong monotonic suppression of final reach with increasing stifling, and a rapid collapse of rumor lifespan once  $p_{SS} > 0\%$ . Spatial structure induces clustering and incomplete penetration, leading to outcomes that can diverge substantially from mean-field expectations. The phase diagrams highlight how transmission and stifling jointly determine whether the rumor saturates the population, persists briefly, or fails to spread widely.

## A Supplementary Results and Diagnostics

### A.1 Monte Carlo consistency check: 1k vs 10k

To verify that the Monte Carlo estimates are not sensitive to the number of repetitions, we repeated the same stifling-probability sweep with 10,000 runs and compared it to the baseline 1,000-run experiment. The two estimates were consistent in the sense that the 10,000-run averages followed the same mean trend as the 1,000-run results at common parameter values (in particular, the high-reach regime at low stifle probability and the progressive drop in reach as stifling increases). The practical effect of increasing the number of runs was mainly to reduce sampling noise (smoother curves / tighter uncertainty), without changing the qualitative conclusions reported in the main text.

### A.2 Temporal dynamics (1k outputs)

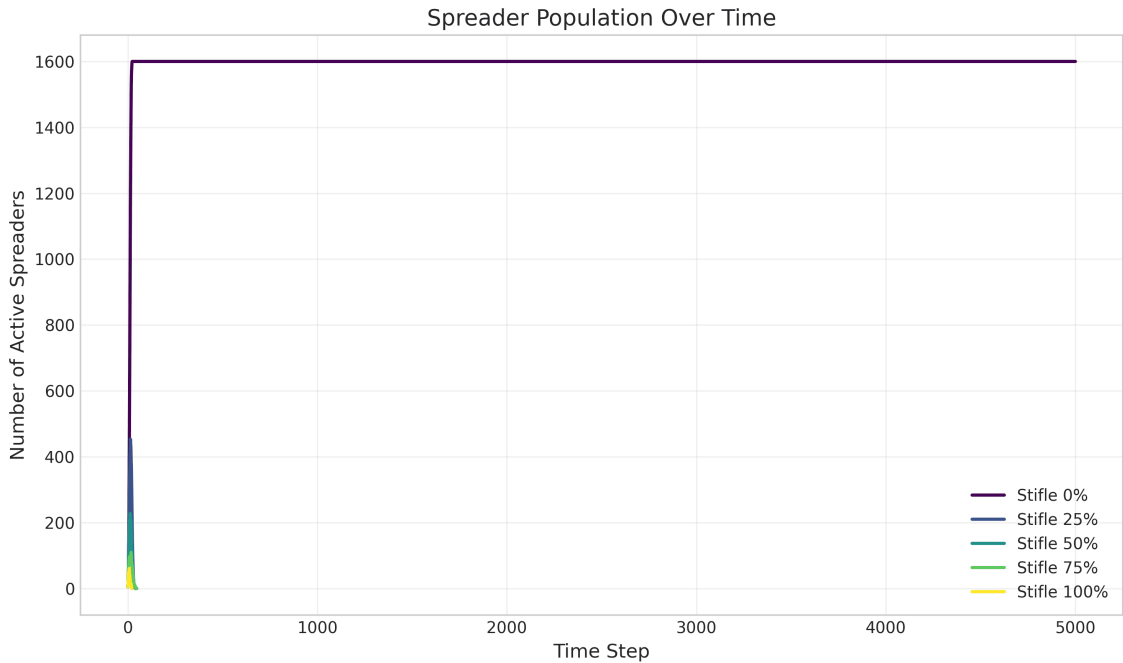


Figure 10: Spreader population over time for several stifle probabilities (1k-run setting). The stifle = 0% case does not extinguish (no stifling mechanism), so the trajectory persists until the imposed simulation horizon (hence the long flat line). For  $s > 0$ , the number of active spreaders peaks early and then collapses as agents transition to the stifler state.

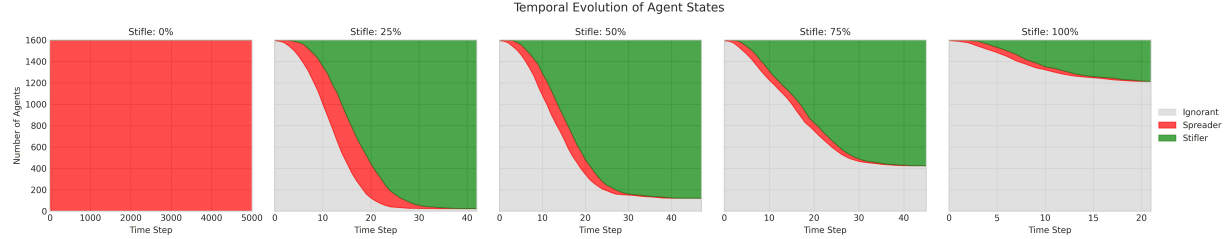


Figure 11: Temporal evolution of the three agent states (Ignorant / Spreader / Stifler) for representative stifle probabilities (1k-run setting). Increasing stifling shortens the spreading phase and leaves a larger remaining ignorant population at termination.

### A.3 Rumor lifespan summary (1k outputs)

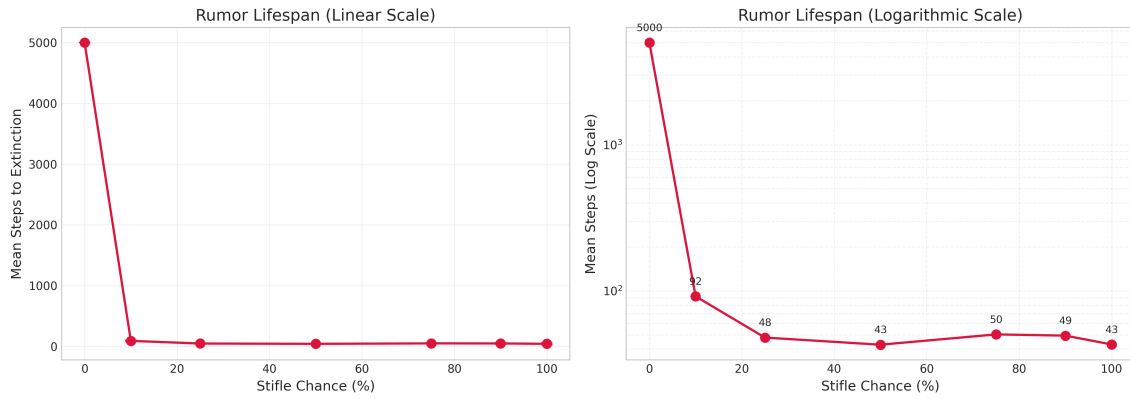


Figure 12: Mean extinction time (rumor lifespan) as a function of stifle probability (1k-run setting), shown on both linear and logarithmic scales. The stifle = 0% case persists to the simulation horizon, whereas even modest stifling yields rapid extinction.

#### A.4 Stochastic variability across simulations (1k outputs)

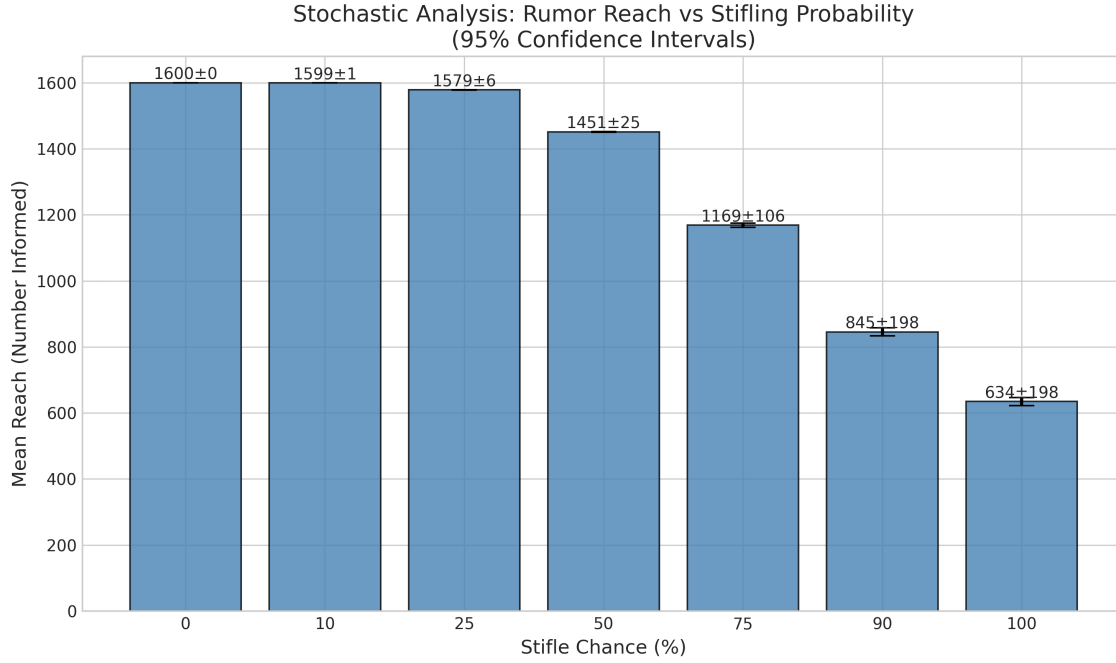


Figure 13: Mean rumor reach (number informed) across simulations, with 95% confidence intervals, as a function of stifle probability (1k-run setting). The plot highlights near-saturation at low stifling and increasing variability as stifling strengthens.

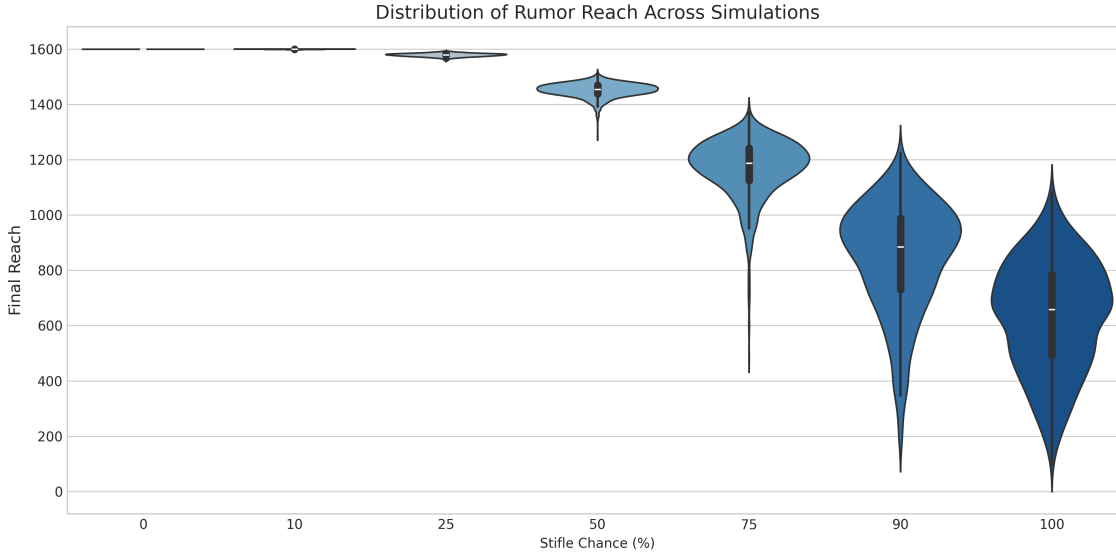


Figure 14: Distribution of final reach across simulations (violin plots) for different stifle probabilities (1k-run setting). The spread of outcomes increases with stifling, indicating stronger stochasticity when spreading is frequently curtailed.

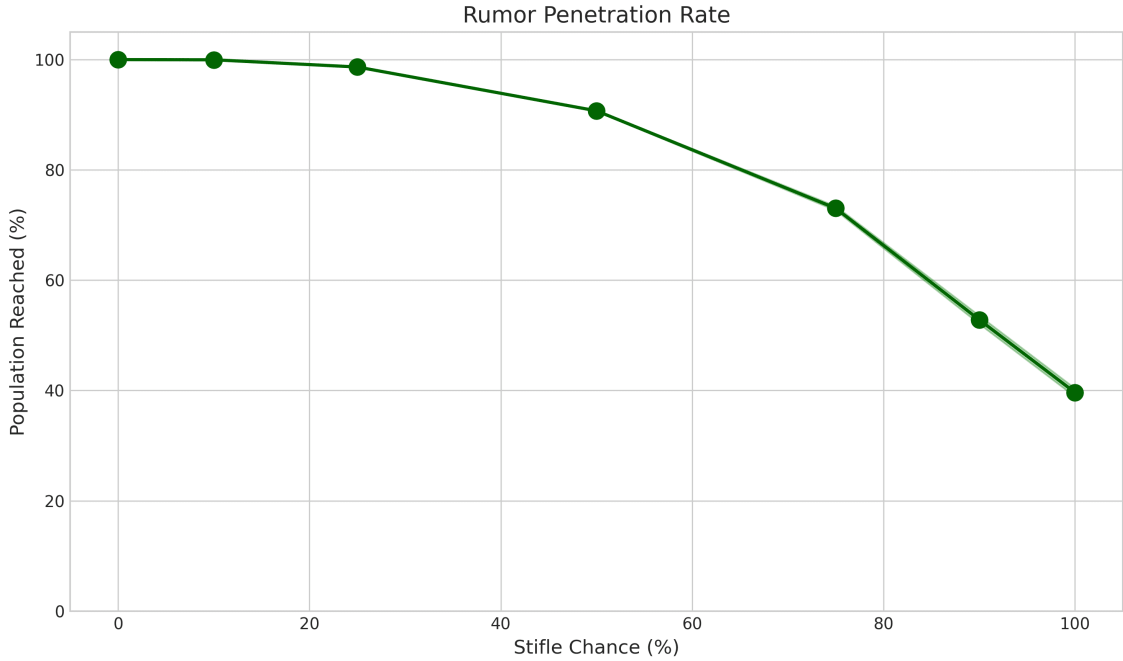


Figure 15: Rumor penetration rate (percentage of population reached) as a function of stifle probability (1k-run setting). This is the reach normalized by the total population size.

### A.5 Two-parameter sensitivity: transmission vs stifling (1k outputs)

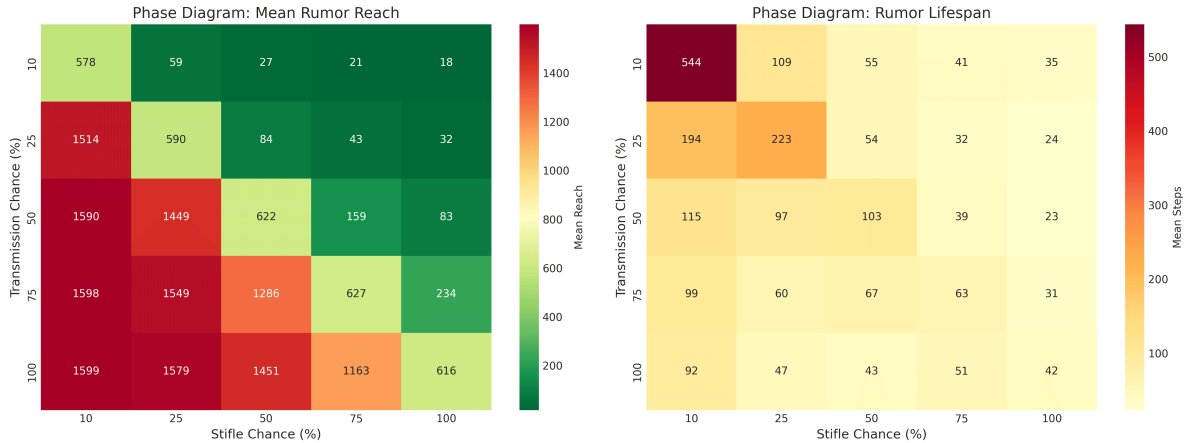


Figure 16: Phase diagrams summarizing (left) mean rumor reach and (right) mean rumor lifespan (mean steps to extinction) over a grid of transmission and stifle probabilities (1k-run setting). Reach increases with transmission and decreases with stifling, while lifespan reflects the competition between spread and termination across the parameter plane.

## A.6 Spatial patterns (1k outputs; representative realizations)

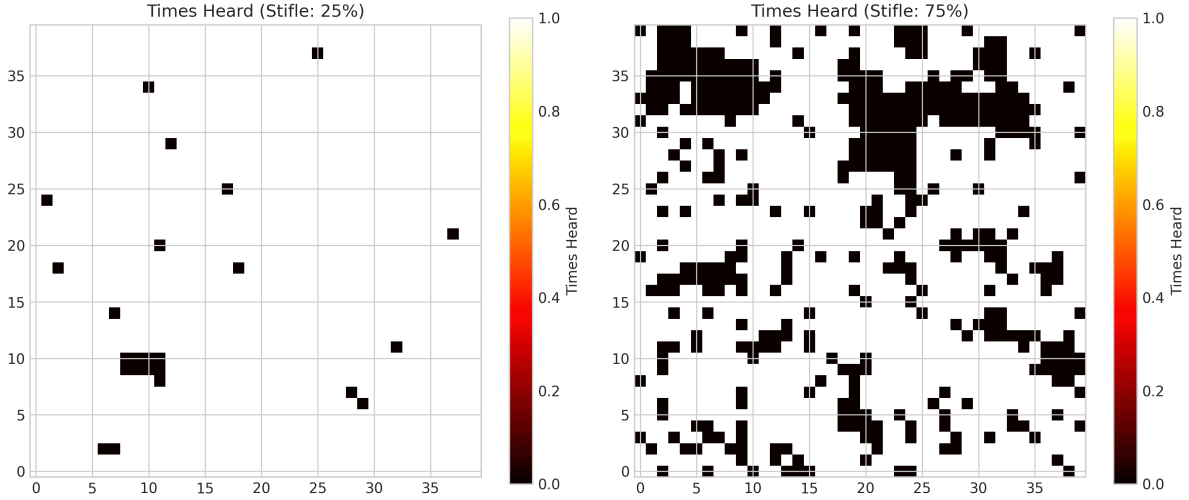


Figure 17: Spatial maps of the “times heard” diagnostic for two representative stifle settings (as displayed in the figure; 1k-run setting). Repeated exposures concentrate in localized neighborhoods rather than being uniformly distributed.

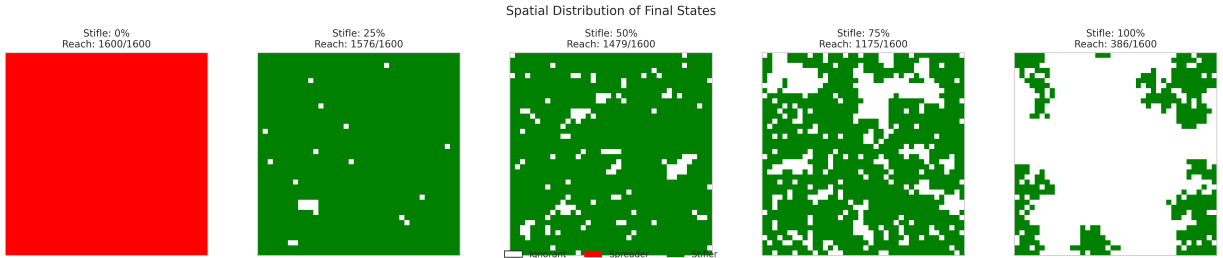


Figure 18: Spatial distribution of final agent states for representative stifle probabilities (panel titles report the realized reach for that run; 1k-run setting). As stifling increases, the final configuration shifts toward larger connected ignorant regions (unreached areas), consistent with the reduced global reach in the aggregate statistics.